

Disruption of White Matter Integrity in the Inferior Longitudinal Fasciculus in Adolescents With Schizophrenia as Revealed by Fiber Tractography

Manzar Ashtari, PhD; John Cottone, PhD; Babak A. Ardekani, PhD; Kelly Cervellione, MA; Philip R. Szeszko, PhD; Jinghui Wu, BS; Steven Chen, BS; Sanjiv Kumra, MD

Context: There is increasing evidence that schizophrenia is characterized by abnormalities in white matter.

Objective: To investigate the integrity of white matter tracts in adolescents with schizophrenia.

Design: Cross-sectional, case-control, whole-brain, voxel-based analysis and fiber tractography using diffusion tensor magnetic resonance imaging.

Setting: University research institute.

Participants: Forty-four individuals (age range, 11-18 years), 23 with a DSM-IV diagnosis of schizophrenia or schizoaffective disorder and 21 demographically similar healthy controls.

Main Outcome Measures: Fractional anisotropy, trace, and radial diffusivity of diffusion tensor and quantitative tractography.

Results: Voxelwise analysis revealed that adolescents with schizophrenia had reduced fractional anisotropy within

the left inferior temporal ($P < .001$) and occipital ($P < .001$) regions. Tractography was performed to extract the left and the right inferior longitudinal fasciculi (ILF). Measuring the mean diffusion indices along the left ILF, patients had significantly reduced fractional anisotropy ($P < .001$) as well as significantly increased radial diffusivity ($P < .001$) and trace ($P = .003$) after adjusting for differences in a measure thought to reflect premorbid intelligence, Wide Range Achievement Test 3 reading scores. Exploratory analyses revealed that patients with a history of visual hallucinations had lower fractional anisotropy in the left ILF ($P = .02$) than patients without visual hallucinations.

Conclusion: Our findings, which benefited from greater image resolution and methodological control than previous studies conducted in adolescents with schizophrenia, provide strong evidence for lower white matter integrity in the left ILF, particularly for patients with a history of visual hallucinations.

Arch Gen Psychiatry. 2007;64(11):1270-1280

Author Affiliations: Department of Psychiatry Research, Zucker Hillside Hospital, Glen Oaks, New York (Drs Ashtari, Cottone, and Szeszko; Ms Wu; and Mr Chen); Nathan Kline Institute for Psychiatric Research, Center for Advanced Brain Imaging, Orangeburg, New York (Dr Ardekani); Department of Clinical Research, Jamaica Hospital Medical Center, Jamaica, New York (Ms Cervellione); and Department of Psychiatry, University of Minnesota, Minneapolis (Dr Kumra).

Dr Ashtari is now with the Radiology Department, The Children's Hospital of Philadelphia, Philadelphia, Pennsylvania.

ADOLESCENTS WITH EARLY-onset schizophrenia (EOS) (defined as onset of psychotic symptoms by age 18 years) provide a unique opportunity to examine regional and disease-specific late abnormal brain development in schizophrenia.¹ Prior anatomical brain magnetic resonance imaging (MRI) studies conducted in EOS have revealed a striking postpsychotic progressive loss of cortical gray matter during adolescence, which could either reflect abnormalities in synaptic pruning or an increase in myelinated white matter.²

Recently, several postmortem studies have found well-replicated alterations in myelin-related gene expression,³⁻⁵ and it is possible that a disruption in myelination or other factors associated with the

development of fiber tracts projecting to different cortical areas could also contribute to the pathophysiology of schizophrenia. To date, several investigators have used diffusion tensor imaging (DTI) to examine white matter integrity in adults with schizophrenia; however, fewer studies have been conducted in adolescents. With some exceptions,⁶⁻⁸ the majority of DTI studies have found reductions in white matter fractional anisotropy (FA) predominantly in adults with chronic schizophrenia, potentially reflecting lower white matter "integrity." The regional specificity of these findings has been inconsistent.^{9,10} Nevertheless, some of the most reproducibly consistent FA differences in schizophrenia have involved the anterior cingulate,¹¹⁻¹⁴ corpus callosum,^{12,15-20} left uncinate fasciculus,^{18,21} left arcuate fasciculus,^{12,18,21} and tem-

Table 1. Subject Demographics

| Variable | Patients With EOS (n=23) | Healthy Controls (n=21) | Statistic | P Value |
|----------------------------------|-----------------------------|----------------------------|------------------|---------|
| Age, y | | | <i>t</i> = .67 | .51 |
| Mean (SD) | 15.8 (1.9) | 15.3 (2.9) | | |
| Range | 11.7-18.2 | 10.2-19.0 | | |
| Sex, No. | | | χ^2 = .08 | .78 |
| Male | 13 | 11 | | |
| Female | 10 | 10 | | |
| Ethnic group, No. | | | χ^2 = 1.59 | .21 |
| White | 12 | 7 | | |
| Nonwhite | 11 | 14 | | |
| Median socioeconomic status, No. | 3 | 3 | χ^2 = 5.22 | .16 |
| Handedness, No. | | | χ^2 = 0.91 | .34 |
| Dextral | 20 | 20 | | |
| Nondextral | 3 | 1 | | |
| WRAT3 score, mean (SD) | 96.5 (16.6) | 110.6 (7.0) | <i>t</i> = -3.44 | <.01 |

Abbreviations: EOS, early-onset schizophrenia; WRAT3, Wide Range Achievement Test 3.

poral and occipital regions.^{15,16,22-25} Overall, these data are, in large part, consistent with a hypothesis that schizophrenia is associated with abnormal connectivity of cortical regions, yet the observed variability across studies could reflect the use of small samples, an interaction of disease and development, patient heterogeneity, or differences in methodology.⁹

Until recently, DTI studies have been confined to voxelwise analysis without establishing any relationship between significant clusters reported. This may have been due to limitations in DTI resolution that have prevented researchers from determining whether clusters of reduced FA are part of the same fiber bundle. Capitalizing on improvements in DTI resolution, fiber tractography is a new and exciting technique that provides researchers with the opportunity to explore whether 2 or more regions of interest (ROIs) are part of the same fiber tract.

The study of adolescents with schizophrenia using DTI offers a unique opportunity to examine a subgroup that is likely to be more homogeneous, in terms of phase of illness and treatment variables, than adults with schizophrenia.⁹ Previously, we demonstrated reduced FA bilaterally in the inferior frontal regions and also in the right occipital region in adolescents with schizophrenia, relative to healthy controls, using an ROI approach.²⁶ Also, we reported reduced FA in the left anterior cingulate region ($P < .001$)²⁷ and in the left posterior superior temporal gyrus and left amygdala regions at a reduced threshold ($P < .01$) using a voxel-based approach.²⁸ However, both studies were limited by the use of a suboptimal acquisition strategy of 5.0-mm slice thickness that may be associated with greater partial volume effects than thin slice acquisition (2.5 mm) and a DTI scheme that in 1 case used 6 diffusion-weighted gradient directions, which may have affected the precision of the DTI measurements.²⁹ Also, our previous method of voxelwise analysis was unable to reveal how areas of lower FA might have been anatomically interconnected. To provide more information about the structural integrity of white matter fiber tracts, the present study used a superior acquisition protocol with thinner slices (2.5 mm) and diffusion tensor fiber tractography.

METHOD

PARTICIPANTS

Twenty-three adolescent patients with EOS and 21 adolescent healthy control (HC) subjects were included in this study. The EOS and HC groups were not significantly different in terms of age, sex, parental socioeconomic status,³⁰ ethnicity, or handedness (**Table 1**). The 2 groups were significantly different in terms of reading decoding scores (Wide Range Achievement Test [WRAT3] reading),³¹ which was used to estimate pre-morbid intelligence in patients. Thus, reading scores were included as a covariate in the appropriate statistical models.

The recruitment and diagnostic procedures have been described in detail elsewhere.^{27,32} Briefly, patients were recruited from inpatient and outpatient units. All patients and their parents were interviewed using portions of the Schedule for Affective Disorders and Schizophrenia for School-Aged Children—Present and Lifetime Version (K-SADS-PL)³³ by a psychologist or psychiatrist (reliability of diagnosis, $\kappa = 0.83$). All patients were diagnosed with schizophrenia ($n = 18$), schizoaffective disorder ($n = 4$), or schizophreniform disorder ($n = 1$). Patients had an average age at onset of psychosis of 13.5 years (range, 8-17 years); duration of illness of 2.4 years (range, 1-7 years); total psychiatric symptom score of 36 (range, 23-54) using the Brief Psychiatric Rating Scale³⁴; total negative symptom score of 38 (range, 1-90; not including attention items) using the Scale for the Assessment of Negative Symptoms³⁵; and chlorpromazine equivalent for antipsychotic dosage at time of scan of 365.5 mg (range, 0-1367 mg).^{36,37}

Healthy control subjects were recruited from the surrounding community and adolescent medical clinics and were also interviewed using portions of the K-SADS-PL. Exclusion criteria for all patients and comparison subjects included a documented history of mental retardation, recent substance use, and any neurological disorders that could potentially affect cognitive development or produce psychotic-like symptoms. In addition, HCs were excluded if they had a history of any major psychiatric disorder or a first-degree relative with bipolar disorder or a psychotic disorder.²⁷

The North Shore—Long Island Jewish Health System institutional review board approved all procedures, including recruitment and consent. Written informed consent or assent was obtained from participants and their legal guardians (for subjects who were younger than 18 years).

MRI APPARATUS AND PROCEDURES

Magnetic resonance examinations were conducted at the Long Island Jewish Medical Center on a 1.5-T GE Neuro Vascular Interactive (NV/i) system (General Electric, Milwaukee, Wisconsin) with high gradient strength of 50 mT/m with the slew rate of 150 T/m/s. The diffusion tensor sequence used in this study used a total of 15 nonparallel diffusion gradient directions and a diffusion sensitization b-factor of 1000 s/mm² for acquisition of 50 isotropic slices (2.5 × 2.5 × 2.5 mm³) through the whole brain. Two b=0 images were acquired with a number of excitations of 2, and all other diffusion images with non-zero b-values in each gradient direction were acquired with 2 averages (number of excitations, 2), increasing the signal-to-noise ratio of the scans. Images were acquired parallel to the anterior-posterior commissures using a dual spin-echo prepared sequence to reduce eddy current-related image geometric distortions³⁸ and a ramp-sampled, spin-echo, single-shot echo planar imaging method with a repetition time of 14 000 milliseconds; echo time, 77 milliseconds; matrix size, 88 × 88 (zero-filled to 256 × 256); field of view, 22 × 22 cm²; slice thickness, 2.5 mm (no gap); number of excitations, 2; and total acquisition time, 8.24 minutes. All images were investigated to be free of motion, ghosting, constant high-frequency lines, and wrap-around artifacts at the time of image acquisition.

In addition to the DTIs, we acquired a matching fast-spin echo (FSE) double-echo sequence (repetition time, 5.5 seconds; echo time, 17 and 102 milliseconds; matrix size, 256 × 192; field of view, 22 × 22 cm²; slice thickness, 2.5 mm with no gap; echo train length, 16; bandwidth, 21 kHz; number of excitations, 2; scan time, 8.78 minutes) as well as a fluid-attenuated inversion recovery (FLAIR) sequence for clinical purposes. Also obtained for registration purposes was a 3-dimensional spoiled gradient-echo (SPGR) sequence with inversion preparation pulse (repetition time, 10.1 milliseconds; echo time, 4.2 milliseconds; bandwidth, 21 kHz; matrix size, 256 × 192; field of view, 22 × 22 cm²; 124 coronal slices; slice thickness, 1.5 mm; inversion time, 600 milliseconds; number of excitations, 1; scan time, 7.44 minutes).

SPATIAL NORMALIZATION

Details of normalization methodology used here were presented in earlier reports.^{27,39,40} Briefly, intersubject and intrasubject registrations were carried out to ensure image alignment prior to vector and voxel averaging. In addition, we implemented an elastic registration algorithm for correction of the echo planar image geometric distortions. The method of distortion correction used was a nonparametric elastic registration algorithm that used cross-correlation as a similarity measure.³⁹ In this algorithm, a subject image (b=0 diffusion T2 image) is elastically deformed to match a target image (T2 FSE image). The algorithm is used for 2 purposes in the present article: distortion correction of the DTI echo planar images and spatial normalization of the subjects' SPGR images. Rigid-body registration was used¹⁶ for intrasubject registration to control for any subtle head motion or possible subject motion that may have occurred between or within sequence acquisitions. A single subject with the median brain volume among all participants was used as the template image. The whole-brain 3-dimensional SPGR of the template image was transformed into Talairach space using the program AFNI (<http://afni.nimh.nih.gov/afni/>). The diffusion-weighted images of each subject were spatially normalized to this template image. To summarize, spatial normalization of the image derived from the DTI data was performed by 3 different registrations: (1) elastic registration of the DTI data to the T2 FSE image to remove spatial distortions;

(2) rigid-body registration of the T2 FSE image and the SPGR image within each subject; and (3) elastic registration of the SPGR image of each subject to a template (target) that had already been transferred into the Talairach space. The transformations from all 3 registrations were combined mathematically into a single transformation and applied to the DTI driven images (eg, axial, radial, mean diffusivity, and eigenvectors) with a single interpolation operation.

Eigenvectors and eigenvalues of the diffusion tensor matrix for each voxel were computed from the 17 DTI volumes (15 gradient directions and 2 b=0 images) for each subject using methods described by Basser⁴¹ and Pierpaoli and Basser.⁴² Using the computed eigenvalues (λ_1 , λ_2 , and λ_3), we calculated the magnitude images for λ_{\perp} [$(\lambda_2 + \lambda_3)/2$] and λ_{\parallel} (λ_1); the trace value of D (apparent diffusion coefficient, $D_{tr} = [(\lambda_1 + \lambda_2 + \lambda_3)]$); and FA. Axial (λ_{\parallel}), radial (λ_{\perp}), mean diffusivity (D_{tr}), and FA maps were transferred into Talairach space using the registration procedures. It should be stressed that the λ_{\parallel} , λ_{\perp} , and FA maps were first computed in the subject's native image coordinates and then transformed into the common Talairach space using the 3-step registration process. All images were smoothed with a 6-mm full-width half-maximum gaussian kernel in 3D. Eigenvectors were used for tractography purposes.

TRACTOGRAPHY PROCEDURES

Fiber tractography was performed using DTIStudio, which is based on the fiber-assignment-by-continuous-tracking method.^{43,44} Fibers are selected based on initiating a seed pixel in the anatomy of choice. From this seed point, a line is propagated that follows the principal eigenvector in 3-dimensional contiguous space from voxel to voxel.⁴⁴ The principal eigenvector is assumed to represent the local fiber direction. Using DTIStudio, tracking the major human fiber bundles is reported to be highly reproducible.⁴⁴⁻⁴⁶ DTIStudio performs fiber tracking only once in the beginning, and when the brute-force fiber tracking is finished, all tracking results are saved, but only a subset of them is visualized on request by user-defined ROIs in the anatomy of interest.

There are 2 thresholds for tractography in the DTIStudio: FA and turning angle (to prevent sharp turns). A threshold of 0.20 for FA value was used to perform tractography. This value was suggested as the optimal FA value for tractography by Mori and colleagues⁴⁴ and Kunimatsu and colleagues.⁴⁷ A second threshold was for the inner product of the 2 consecutive vectors to be greater than 0.75, which prohibits the turning of angles larger than 41° during tracking.^{45,46} A more detailed description of DTIStudio and its functions is presented in a recent article by Jiang and colleagues.⁴⁸

In the present report, Talairach-transferred principal eigenvectors and FA images were used as input to DTIStudio to construct the fiber bundles. The OR function of DTIStudio extracts all the tracts that pass through a single defined ROI. To perform tractography, a seed ROI is used in conjunction with the OR function to extract the white matter fibers of interest. Anatomical information and color DTI images were used to accurately differentiate the selected fibers from the neighboring white matter tracts. On the color maps, the colors red, green, and blue were assigned to the right-left, anterior-posterior, and superior-inferior orientations, respectively.⁴⁹

Three white matter fiber bundles of the left and right ILF and anterior corpus callosum were extracted as part of the present report. The seed ROI for the left ILF was selected based on the approximate location of the medial temporal lobe FA abnormality on 1 slice. A similar location in the right middle temporal area was used to place the seed ROI for the right ILF. Selection of the ROI for the extraction of the anterior callosal fibers

was based on a recent report by Sullivan and colleagues⁵⁰ on the corpus callosum and its cortical connectivity. We used the anterior segment of the midsagittal corpus callosum as the seed ROI to extract the callosal fibers connecting to the prefrontal brain areas as the control fibers of the study.

GROUP AVERAGING OF DIFFUSION TENSOR DATA FOR TRACTOGRAPHY

To perform tractography, whether for a single subject or for averaged data from all participants, DTIStudio requires a scalar field representing the FA and a vector field representing the principal eigenvector of the diffusion tensor. Therefore, to perform tractography on group data, we specified the average FA and the “average” principal eigenvector for all subjects. Using the rigorous registration procedure described here and in our earlier reports,^{24,40} we obtained a deformation field specific to each subject that could be used for spatial normalization of the subject’s DTI images to a standardized space (Talairach). This deformation field is a vector-valued function of a vector variable that maps the coordinates of any given grid point in the standardized space to its corresponding point in the subject’s original DTI image space.³⁹ To obtain the group-averaged FA image in Talairach space, we simply applied the deformation field of each subject to the FA image and then took the arithmetic average of all spatially normalized FA images to yield the average FA in Talairach space for the group.

Attainment of a principal eigenvector field representing the group is more complicated than the procedure described here for obtaining the average FA. The principal eigenvector field for the group was obtained by first computing the Jacobian matrix⁵¹ of the deformation field at each grid point on the standardized space for each subject. The eigenvector in each subject’s original DTI image space that would be mapped to the particular grid point in the standardized space was then reoriented by premultiplying it with the computed Jacobian, as suggested by Alexander et al.⁵² It should be mentioned that because DTIStudio only uses the principal eigenvector to perform tractography, we did not apply reorientation to the remaining 2 radial eigenvectors. Reorientation of the principal eigenvector was subsequently repeated for all subjects at all grid points in the standardized space. Thus, for each grid point, we obtained as many (reoriented) eigenvectors as there were subjects in the study (N=44). Finally, at each grid point, a principal component analysis⁵³ was performed on the 44 eigenvectors. The principal eigenvector of this analysis was then taken to represent the whole group at the grid point in question.

STATISTICAL ANALYSES

Demographic differences between patients with EOS and HCs were analyzed using independent sample *t* tests and χ^2 tests as appropriate. Voxelwise analysis of covariance (VANCOVA) was used to perform the voxelwise analysis. We controlled for type I errors (false positives) using the false discovery rate (FDR) measure⁵⁴ of the ‘fdr’ program supplied by the FSL software package (<http://www.fmrib.ox.ac.uk/fsl/>). The FDR measure represents the expected proportion of rejected hypotheses that are false positives. For FDR=0.01, the ‘fdr’ program yielded *P* values of .00732, .00744, and .00742 for the FA, radial diffusivity, and the trace maps, respectively. Thus, we selected a conservative *P* value threshold of $P < .001$ for our analysis that ensures a false discovery rate of less than 1% (FDR<0.01). As an additional safeguard against false positives, we only retained clusters larger than 100 voxels in size. We performed an ANCOVA test between patients with EOS and HCs on the

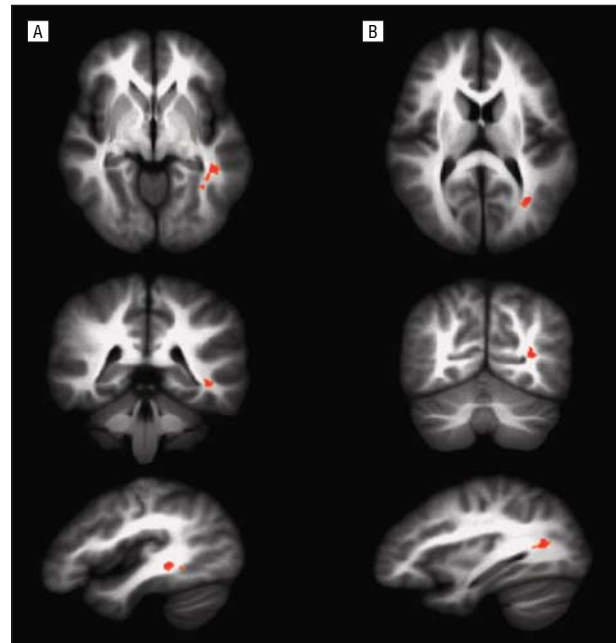


Figure 1. Voxelwise analysis of covariance shows decreased fractional anisotropy (FA) for 100 or more contiguous voxels at $P < .001$ superimposed on the averaged Talairach transferred images of all subjects. Reduced FA clusters are depicted along the left inferior temporal lobe (A) and the left occipital area (B).

average diffusion parameter for all extracted fibers. All statistical analyses were executed using SPSS 11.0 (SPSS Inc, Chicago, Illinois) or Stata (StataCorp, College Station, Texas).

RESULTS

VOXELWISE ANALYSIS

We performed VANCOVA to assess water diffusion changes in patients with EOS relative to HCs, controlling for an estimate of premorbid intelligence (ie, WRAT3 reading scores). Areas of lower FA are presented as yellow clusters superimposed on the averaged 3-dimensional SPGR images of all 44 subjects. At a high threshold of statistical significance ($P < .001$) and a cluster size extent threshold of 100 or more contiguous voxels, 2 clusters with decreased FA were identified in the left hemisphere in the inferior temporal and occipital regions (**Figure 1**). Whole-brain voxelwise analysis did not show any areas of the brain with increased FA for patients with EOS relative to HCs. A summary of findings with their Talairach coordinates and cluster sizes is presented in **Table 2**.

Similar VANCOVA analyses (controlling for WRAT3 reading scores) at the same statistical threshold ($P < .001$) and extent threshold of 100 or more voxels were performed for the axial and radial diffusivity and trace images. Increased radial diffusivity (λ_{\perp}) was observed (**Figure 2**) in the same brain areas of the left inferior temporal and the left occipital areas that showed decreased FA (Figure 1 and Figure 2). The 2 clusters of increased radial diffusivity in columns 1 and 2 were reported as 1 continuous connected cluster in the VANCOVA analysis. There were no changes in the axial

Table 2. Talairach Coordinates and Voxelwise Analysis Results of Fractional Anisotropy, Radial (λ_{\perp}), and Trace (D_{tr}) Parameters of Patients With EOS (n=23) Relative to Healthy Controls (n=21)

| Changes in Diffusion Parameters | Anatomical Location | Cluster Size (No. of Connected Voxels) | x | y | z |
|-------------------------------------|---|---|-----|-----|----|
| Decreased FA cluster 1 | Left fusiform gyrus region, subgyral, white matter | 453 | -37 | -40 | 0 |
| Decreased FA cluster 2 | Left gyrus occipitalis medius, subgyral, white matter | 192 | -30 | -59 | 15 |
| Increased λ_{\perp} cluster | Left fusiform gyrus region, subgyral, white matter | 3664 | -35 | -43 | 3 |
| Increased D_{tr} cluster | Left fusiform gyrus region, subgyral, white matter | 2363 | -35 | -41 | 1 |

Abbreviations: EOS, early-onset schizophrenia; FA, fractional anisotropy.

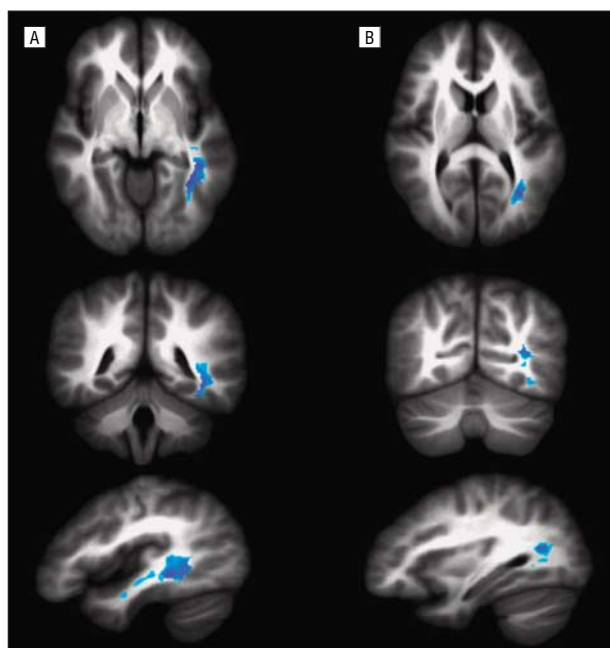


Figure 2. Voxelwise analysis of covariance shows increased radial diffusivity (λ_{\perp}) in 100 or more contiguous voxels at $P < .001$ superimposed on the averaged Talairach transferred images of all subjects. Increased radial diffusivity is depicted along the left inferior temporal lobe (A) and the left occipital area (B).

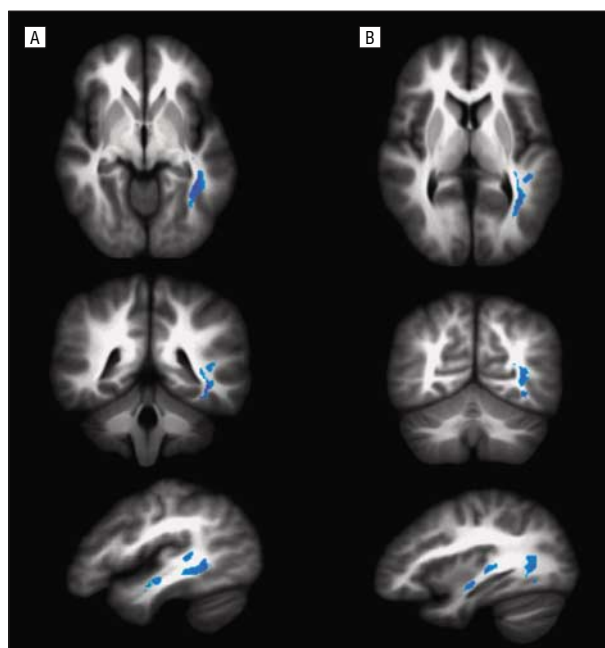


Figure 3. Voxelwise analysis of covariance shows increased trace (D_{tr}) in 100 or more contiguous voxels at $P < .001$ superimposed on the averaged Talairach transferred images of all subjects. Increased trace is depicted along the left inferior and superior temporal lobe (A) and the left occipital area (B).

diffusivity (λ_{\parallel}) in the same areas of decreased FA and increased λ_{\perp} . At the same statistical threshold of $P < .001$ and extent threshold of 100 or more voxels, VANCOVA analysis (controlling for WRAT3 reading scores) for trace images (D_{tr}) revealed increased trace values in the same brain region that had decreased FA and increased λ_{\perp} (**Figure 3**). Similar to the radial diffusivity clusters, the 2 clusters of increased trace (D_{tr}) in Figure 3 were reported as 1 continuous cluster in the VANCOVA analysis. A summary of findings with their respective Talairach coordinates and cluster sizes is presented in Table 2.

TRACT-SPECIFIC MEASUREMENTS

The left ILF was extracted using the approximate location of the reduced FA cluster located in the inferior temporal lobe as a guide for the placement of the tractography seed ROI. The medial temporal abnormal FA cluster was 453 voxels in size (Table 2) and extended over 14 slices. The seed ROI was a small in-plane ROI (approximate size of 57 pixels) placed only on 1 slice in the me-

dial temporal lobe. Using this ROI in conjunction with the OR function of DTIStudio, we extracted the left ILF fiber bundle (**Figure 4** and **Figure 5**). Therefore, the extraction of the ILF fiber bundle was independent from the 2 abnormal FA clusters.

Subsequent to the extraction of the ILF, a visual examination of the 2-dimensional slices in the sagittal, coronal, and axial orientations presented in DTIStudio confirmed that the locations of the 2 abnormal FA clusters lie along the left ILF fiber tract (Figure 4B and D). Because the eigenvector images (Figure 4A and B) and the eigenvalue images (Figure 4B and D) were all transferred to the same common Talairach space, locations of the reduced FA clusters were easily identifiable and corresponded to the same slices with abnormal diffusion indices (Figures 1-4). Assuming that the ILF is involved in higher-order human visual processing and that vision is fundamentally a bilateral process, we also extracted the right ILF fibers (using a similar location for the seed ROI in the right medial temporal lobe) and obtained the diffusion values using the Talairach transferred images.

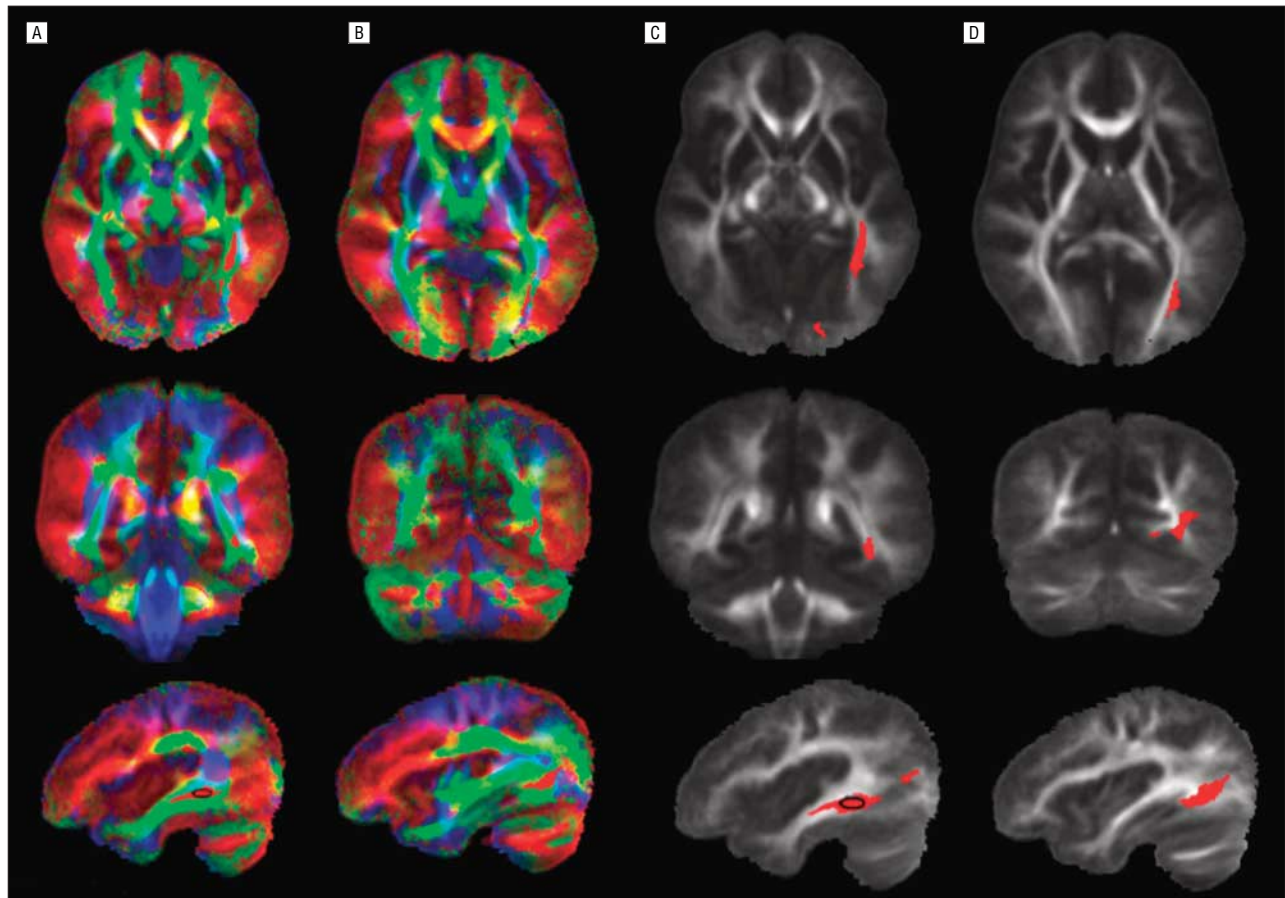


Figure 4. Based on voxelwise analysis results, a single region of interest is placed onto medial temporal area (black ellipsoid on sagittal image) to extract the inferior longitudinal fasciculi fiber bundle. The gray scale (C and D) and color images (A and B) are the Talairach transferred averaged fractional anisotropy and principal eigenvector of all subjects, respectively.

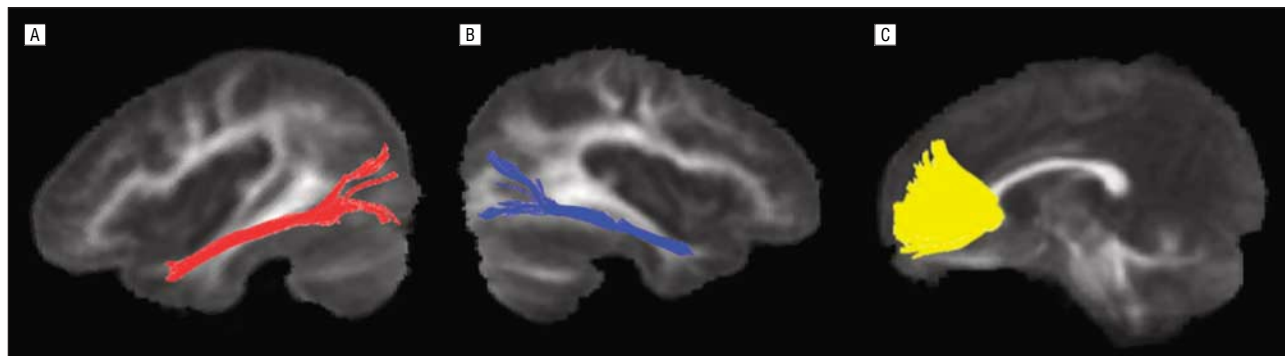


Figure 5. The left (A) and right (B) inferior longitudinal fasciculi (ILF) fiber bundles and anterior callosal connections to the prefrontal brain areas (used as the control tract) (C) are reconstructed using the DTIStudio tractography program. Fibers are superimposed onto the Talairach transferred averaged fractional anisotropy (FA) of all 44 subjects. These images demonstrate that ILF fibers occupy extensive areas with its branches penetrating the occipital and temporal cortices.

To quantify tract-specific changes of the extracted fiber pathways, we extracted scalar values of diffusion parameters and FA for individual subjects. To obtain these scalar values, we used the resultant ILF and the control tracts (Figure 5) as a specific anatomical ROI to be merged with the Talairach transferred FA, axial, radial, and average diffusivity images of each subject. Because the vector and scalar images were all coregistered in Talairach space, specific tract measurements were easily acquired using software developed in house.

TRACTOGRAPHY RESULTS

The left and the right ILF and a tract composed of anterior callosal fibers projecting to the prefrontal cortex (used as the control tract) were extracted 10 times using the procedure and DTIStudio (the software of choice for tractography). The tract-specific fibers were superimposed as an anatomical ROI onto the Talairach-transferred FA, λ_{\parallel} , λ_{\perp} , and D_{tr} images to obtain the scalar values for their respective diffusion parameters. Results of the

Table 3. Mean of 10 ILF-Extracted Tract-Specific Measurements of Diffusion Indices and Statistical Analysis Between Patients With EOS and Healthy Controls

| Fiber Bundle Diffusion Measures ^a | Mean (SD) ^b | | Test Statistic ^c | P Value |
|--|-------------------------|--------------------------|-----------------------------|---------|
| | Healthy Controls (n=21) | Patients With EOS (n=23) | | |
| Left ILF | | | | |
| Fractional anisotropy | 326.57 (23.79) | 294.79 (17.83) | 23.93 | < .001 |
| Radial diffusivity (λ_{\perp}) | 773.74 (44.20) | 836.18 (36.48) | 18.68 | < .001 |
| Axial diffusivity (λ_{\parallel}) | 1287.72 (60.17) | 1315.33 (42.04) | 0.72 | .40 |
| Trace (D_{tr}) | 2835.21 (137.13) | 2987.69 (107.42) | 10.33 | .003 |
| Right ILF | | | | |
| Fractional anisotropy | 256.57 (36.95) | 245.63 (24.75) | 2.64 | .11 |
| Radial diffusivity (λ_{\perp}) | 843.11 (45.44) | 870.07 (44.13) | 2.77 | .10 |
| Axial diffusivity (λ_{\parallel}) | 1242.61 (53.14) | 1261.56 (43.60) | .06 | .82 |
| Trace (D_{tr}) | 2928.82 (112.17) | 3001.69 (240.60) | 1.92 | .17 |
| Prefrontal CC tracts | | | | |
| Fractional anisotropy | 364.59 (31.25) | 350.14 (19.50) | 2.59 | .12 |
| Radial diffusivity (λ_{\perp}) | 775.52 (100.10) | 816.98 (78.45) | 1.38 | .25 |
| Axial diffusivity (λ_{\parallel}) | 1399.72 (138.04) | 1434.39 (86.82) | .39 | .54 |
| Trace (D_{tr}) | 2950.76 (333.19) | 3068.34 (240.60) | .95 | .34 |

Abbreviations: CC, corpus callosum; EOS, early-onset schizophrenia; ILF, inferior longitudinal fasciculi.

^aTen measurements were made with arbitrary units.

^bAll diffusion parameters were multiplied by 1000.

^cAll analyses were performed using analysis of covariance, controlling for Wide Range Achievement Test 3 reading scores.

ANCOVA analyses comparing the FA, λ_{\parallel} , λ_{\perp} , and D_{tr} values of patients with EOS with those of HCs (controlling for WRAT3 reading score) are presented in **Table 3**. Patients with EOS showed decreased FA for the left ILF tract ($P < .001$) and at a trend level for the right ILF ($P = .11$). Patients showed a significant increase in λ_{\perp} for the left ILF ($P < .001$) and a trend level for the right ILF ($P = .10$). Patients showed a significant increase in D_{tr} for the left ILF ($P < .003$). There were no significant differences in λ_{\parallel} for the left ($P = .40$) or the right ($P = .82$) ILF. We did not find significant diffusion parameter differences in the anterior callosal fibers for the patients with EOS relative to HCs.

CLINICAL ANALYSES

As an a posteriori set of exploratory analyses, we compared the tractography values for average FA, λ_{\perp} , λ_{\parallel} , and D_{tr} between patients with ($n = 9$) and without ($n = 14$) a history of visual hallucinations using independent samples t tests. This set of analyses was conducted for values from each extracted tract (ie, the left ILF, right ILF, and tract of anterior callosal fibers). Because the ILF is associated with visual processing,⁵⁵⁻⁵⁸ we hypothesized that patients with a history of visual hallucinations would have significant abnormalities in the diffusion indices of the ILF fiber bundles as compared with patients without a history of visual hallucinations. We further hypothesized that there would be no significant differences in FA, λ_{\perp} , λ_{\parallel} , and D_{tr} in the tract of anterior callosal fibers between these 2 groups because this tract is not thought to be associated with visual processing.

The patient subgroups with and without a history of visual hallucinations were not significantly different

($P < .05$) in terms of demographic or clinical variables. Relative to patients without a history of visual hallucinations, patients with a history of visual hallucinations had significantly lower mean FA in the left ILF ($P = .02$), and a trend was observed for λ_{\perp} in the expected direction (**Table 4**). Although differences between groups in D_{tr} did not reach significance, group differences were in the expected direction. There were no significant differences between groups in λ_{\parallel} . None of the diffusion measures for the right ILF or tract of anterior callosal fibers were significantly different between patients with and without a history of visual hallucinations.

COMMENT

In the present study, we used voxelwise analysis and tractography to compare the white matter fiber tract integrity of adolescents with EOS to HCs. The first set of analyses using VANCOVA revealed 2 clusters of decreased FA within the left middle temporal and left occipital areas of patients with EOS relative to HCs. In addition, patients with EOS had increased radial diffusivity and increased trace values in the same brain regions where decreased FA was observed. The subsequent independent tractography assessment confirmed that the 2 abnormal FA clusters were located along the path of the left ILF connecting the occipital and temporal cortex in the left hemisphere. Statistical analysis of the diffusion parameters of the left ILF for the entire sample ($N = 44$) showed a similar pattern of abnormality, as was found in the voxelwise analysis. Furthermore, our finding of lower white matter "integrity" within the left ILF had an important clinical correlate: patients with EOS with visual hallucinations demonstrated significant lower FA in the left ILF

Table 4. Differences in Diffusion Measures of the Left and Right ILF and the Prefrontal Corpus Callosum Fiber Tracts Between Patients With and Without a History of Visual Hallucinations

| Fiber Bundle Diffusion Measures ^a | Mean (SD) ^b | | Test Statistic ^c | P Value |
|--|---|---|-----------------------------|---------|
| | Patients Without Visual Hallucinations (n=14) | Patients With Visual Hallucinations (n=9) | | |
| Left ILF | | | | |
| Fractional anisotropy | 301.55 (17.92) | 284.28 (12.19) | 2.53 | .02 |
| Radial diffusivity (λ_{\perp}) | 825.49 (36.45) | 852.81 (31.46) | -1.85 | .08 |
| Axial diffusivity (λ_{\parallel}) | 1312.01 (42.84) | 1320.50 (42.78) | -.46 | .65 |
| Trace (D_{tr}) | 2962.99 (108.41) | 3026.11 (99.52) | -1.41 | .17 |
| Right ILF | | | | |
| Fractional anisotropy | 251.48 (24.06) | 236.53 (24.31) | 1.45 | .16 |
| Radial diffusivity (λ_{\perp}) | 862.18 (46.20) | 882.34 (40.10) | -1.07 | .29 |
| Axial diffusivity (λ_{\parallel}) | 1262.78 (50.80) | 1259.67 (32.04) | -.16 | .87 |
| Trace (D_{tr}) | 2987.12 (132.66) | 3024.35 (100.19) | -.72 | .48 |
| Prefrontal CC tracts | | | | |
| Fractional anisotropy | 354.75 (19.27) | 342.97 (18.64) | 1.45 | .16 |
| Radial diffusivity (λ_{\perp}) | 802.99 (90.25) | 838.74 (53.03) | -1.07 | .29 |
| Axial diffusivity (λ_{\parallel}) | 1425.05 (101.84) | 1448.91 (59.05) | -.63 | .53 |
| Trace (D_{tr}) | 3031.02 (279.45) | 3126.39 (161.47) | -.93 | .37 |

Abbreviations: CC, corpus callosum; ILF, inferior longitudinal fasciculi.

^aTen measurements were made using arbitrary units.

^bAll diffusion parameters were multiplied by 1000.

^cAll analyses were performed using independent sample *t* tests.

compared with patients who reported never having experienced visual hallucinations.

Because human visual processing is fundamentally bilateral, we performed additional tractography in the right hemisphere, which led to the extraction of the right ILF. We investigated whether diffusion parameters of the right ILF differed significantly between groups and its relation to visual hallucination in patients with and without a history of visual hallucinations. Overall, our results suggest group differences between patients and HCs in the right ILF; however, these differences did not reach statistical significance, perhaps reflecting small sample size or that the pathological process resulting in lower anisotropy is asymmetric and initially affects the left hemisphere in the disease process.

To provide divergent validity and specificity to our findings, we extracted a tract of anterior callosal fibers projecting to prefrontal brain regions as the control tract because this tract is not thought to be associated with visual processing, to our knowledge. Analysis of the control tract showed no significant differences in any of the diffusion parameters between groups (patients with EOS and HCs) and no significant differences in values of the diffusion parameters between patients with and without a history of visual hallucinations.

In sum, our analyses revealed a pattern of decreased diffusion anisotropy within the occipital and temporal regions, similar to what has been reported in adults with both chronic^{12,15,16,22,25} and first-episode schizophrenia.^{23,24} We should emphasize, however, that the present study has a number of advantages over our previous pilot studies^{26,27}: (1) we acquired images from thin, 2.5-mm slices (as opposed to 5-mm slices in the previous studies), which reduced the possibility of partial volume effects; (2) we implemented a tractography proto-

col; (3) our present study used a more homogeneous sample (ie, adolescents with EOS) than our previous studies with adults; and (4) we included a broader range of diffusion measures (ie, axial diffusivity, radial diffusivity, and trace) to characterize the white matter abnormalities.

Overall, these findings of abnormalities in white matter microstructure in occipital and temporal regions potentially extend previous structural neuroimaging data, which have described cortical thinning in the left occipital lobe in first-episode patients with schizophrenia.⁵⁹ However, the relationship between abnormalities in white and gray matter in patients with schizophrenia remains unclear at present, and longitudinal studies are needed to examine the evolution of white and gray matter pathology in adolescents with schizophrenia.

It has been suggested that the pathophysiologic processes responsible for the observed reductions in anisotropy in patients with schizophrenia could include decreased myelination, a decrease in the number or density of axons, diminished coherence of the measured fiber tract, or an increase in the number or density of fiber tracts perpendicular to the measured tract.¹¹ We believe that the results obtained using the diffusion measures of trace (D_{tr}) and radial diffusivity (λ_{\perp}) provide some insight on the issue of what the observed group differences in our study might mean. Specifically, the FA reductions observed in patients, which were accompanied by increases in trace (suggesting diminished fiber density within the ILF¹¹) and increases in radial diffusivity, suggest a pattern of myelination deficits within the axons of the ILF.⁶⁰ These data are consistent with studies using both electron microscopy⁶¹ and microarray techniques⁵ that have revealed oligodendroglial dysfunction in adults with schizophrenia.

Postmortem studies suggest that there is ongoing myelination in the temporal lobes during the second decade of life in healthy individuals,⁶² and it is possible that a delay in myelination in the ILF might increase susceptibility for developing psychosis in patients at risk for schizophrenia. In typically developing children and adolescents between 6 and 19 years of age, developmental changes in white matter FA values in the occipital cortex (Talairach coordinates: $x=-40, y=-72, z=7$) have been observed using DTI.⁶³ These developmental changes in white matter microstructure could be related to the ability to maintain enduring characteristics of visually presented objects, which continues to evolve during the same time period.⁶⁴ Although Barnea-Goraly and colleagues⁶³ did not use DTI tractography in their recent study to delineate specific fiber tracts, the location of their findings would appear to correspond to the portion of the ILF that extends into the occipital cortex.

Although the specific functions of the ILF remain unclear, recent findings indicate that the ILF appears to mediate the fast transfer of visual signals forward from the occipital cortex to the parahippocampal gyrus and neuromodulatory projections from the amygdala back to early visual areas.⁵⁵ Regarding the latter, it has been suggested that the ILF may be responsible for transmitting signals back to early visual areas pertaining to the salience of visual stimuli so that the visual processing of emotionally significant stimuli may be enhanced.⁵⁵ Thus, it has been hypothesized⁶³ that improved occipital-temporal connectivity may contribute to developmental and individual differences in social cognition; the refinement of form, face, and object representations⁶⁵; and visual-spatial integration.^{64,66} Future studies could examine whether the structural abnormalities of the occipital-temporal pathway that we observed in adolescents with EOS account for any of the social competence deficits observed in adolescents in the early phases of a schizophrenic illness⁶⁷ and impairments in the ability to recognize and respond to emotional facial expressions, as reported for adults with schizophrenia.⁶⁸⁻⁷⁰

Visual hallucinations are commonly reported in adolescents with childhood-onset schizophrenia (ie, 79%),⁷¹ and 39% of the adolescents in our sample with EOS also reported this feature of their illness in addition to other psychotic symptoms. In our sample, adolescents with a history of visual hallucinations had significantly lower FA in the extracted whole fiber tract (ie, left ILF) than adolescents without visual hallucinations. Although highly speculative, it is possible that alterations in white matter microstructure may contribute to low-level visual deficits, such as reduced contrast sensitivity and color discrimination, which have been observed in adults with schizophrenia.²² These deficits may in turn lead to partial visual deprivation and result in patients using previously recorded percepts to fill in sensory gaps,⁷² thus yielding visual hallucinations. Of interest, our finding of reduced FA in the extracted whole fiber tract (ie, the left ILF) in patients with visual hallucinations (relative to patients without visual hallucinations) is somewhat contrary to the report by Hubl and colleagues¹⁸ of higher FA in patients with auditory hallucinations (relative to patients without auditory hallucinations), primarily in the

left arcuate fasciculus and cingulate bundle. However, besides differences in hallucination type (ie, visual vs auditory), our patients (adolescents) were much younger than the patients studied by Hubl and colleagues (older adults), and it is possible that the pathology underlying these perceptual disturbances may be different or due to various other factors.

In light of our findings, there are a number of limitations that need to be addressed. Our sample was relatively small, but this is a problem inherent in the study of early-onset patients, which may account for approximately 5% of cases with schizophrenia.¹ Second, the use of a 15-direction diffusion sequence may not be optimal for tractography. However, our clinical MR system is limited regarding the total number of slices acquired in a given sequence. Therefore, using thin isotropic slices to cover the whole brain, the system's maximum allowable gradient direction was 15. Third, as with all DTI assessments using voxelwise (as opposed to ROI) methodology, there is a potential for type I error; however, white matter abnormalities in patients with schizophrenia are likely to be subtle and could be easily missed using ROI methods. Fourth, choosing a single subject with the median brain (potentially either a patient or HC) as the template image may create a bias in this pediatric study. Nevertheless, we believe that from the options available to us in arriving at a template image, we selected a reasonable course of action. Fifth, although fiber tractography is a promising new procedure for examining white matter pathology, there is no agreement on a single method for extracting tracts of interest. In the current study, we used a single seed point to guide the extraction of fiber tracts and a different extraction method may have yielded different results. It should also be noted that diffusion studies in general may suffer from errors due to misregistration of images caused by eddy current distortion, gradient nonlinearities, subject motion, and susceptibility artifacts.³² Lastly, the size of the abnormal clusters of FA that we detected in the temporal and occipital regions were large, and because the ILF is narrow and abuts the optic radiations for some of its length, it is possible that the abnormalities we observed extend to the optic radiations and are not isolated to the ILF.

Submitted for Publication: September 27, 2006; final revision received April 25, 2007; accepted May 14, 2007.

Correspondence: Manzar Ashtari, PhD, Radiology Department, The Children's Hospital of Philadelphia, 34th Street and Civic Center Boulevard, Philadelphia, PA 19104 (ashtari@email.chop.edu).

Financial Disclosure: None reported.

Funding/Support: This study was supported in part by grants MH-070612 (Dr Ashtari), 1RO1-MH073150-01A2 (Dr Kumra), and 7K23MH64556-06 (Dr Kumra) from the National Institute of Mental Health (NIMH).

REFERENCES

1. Rapoport JL, Addington AM, Frangou S, Psych MR. The neurodevelopmental model of schizophrenia: update 2005. *Mol Psychiatry*. 2005;10(5):434-449.
2. Gogtay N, Giedd JN, Lusk L, Hayashi KM, Greenstein D, Vaituzis AC, Nugent TF III, Herman DH, Clasen LS, Toga AW, Rapoport JL, Thompson PM. Dynamic map-

- ping of human cortical development during childhood through early adulthood. *Proc Natl Acad Sci U S A*. 2004;101(21):8174-8179.
3. Davis KL, Stewart DG, Friedman JI, Buchsbaum M, Harvey PD, Hof PR, Buxbaum J, Haroutunian V. White matter changes in schizophrenia: evidence for myelin-related dysfunction. *Arch Gen Psychiatry*. 2003;60(5):443-456.
 4. Katsel P, Davis KL, Gorman JM, Haroutunian V. Variations in differential gene expression patterns across multiple brain regions in schizophrenia. *Schizophr Res*. 2005;77(2-3):241-252.
 5. Katsel P, Davis KL, Haroutunian V. Variations in myelin and oligodendrocyte-related gene expression across multiple brain regions in schizophrenia: a gene ontology study. *Schizophr Res*. 2005;79(2-3):157-173.
 6. Steel RM, Bastin ME, McConnell S, Marshall I, Cunningham-Owens DG, Lawrie SM, Johnstone EC, Best JJ. Diffusion tensor imaging (DTI) and proton magnetic resonance spectroscopy (1H MRS) in schizophrenic subjects and normal controls. *Psychiatry Res*. 2001;106(3):161-170.
 7. Wang F, Sun Z, Du X, Wang X, Cong Z, Zhang H, Zhang D, Hong N. A diffusion tensor imaging study of middle and superior cerebellar peduncle in male patients with schizophrenia. *Neurosci Lett*. 2003;348(3):135-138.
 8. Begre S, Federspiel A, Kiefer C, Schroth G, Dierks T, Strik WK. Reduced hippocampal anisotropy related to anteriorization of alpha EEG in schizophrenia. *Neuroreport*. 2003;14(5):739-742.
 9. Kanaan RA, Kim JS, Kaufmann WE, Pearson GD, Barker GJ, McGuire PK. Diffusion tensor imaging in schizophrenia. *Biol Psychiatry*. 2005;58(12):921-929.
 10. Kubicki M, McCarley R, Westin CF, Park HJ, Maier S, Kikinis R, Jolesz FA, Shenton ME. A review of diffusion tensor imaging studies in schizophrenia. *J Psychiatr Res*. 2005;41(1-2):15-30.
 11. Kubicki M, Westin CF, Nestor PG, Wible CG, Frumin M, Maier SE, Kikinis R, Jolesz FA, McCarley RW, Shenton ME. Cingulate fasciculus integrity disruption in schizophrenia: a magnetic resonance diffusion tensor imaging study. *Biol Psychiatry*. 2003;54(11):1171-1180.
 12. Kubicki M, Park H, Westin CF, Nestor PG, Mulkern RV, Maier SE, Niznikiewicz M, Connor EE, Levitt JJ, Frumin M, Kikinis R, Jolesz FA, McCarley RW, Shenton ME. DTI and MTR abnormalities in schizophrenia: analysis of white matter integrity. *Neuroimage*. 2005;26(4):1109-1118.
 13. Sun Z, Wang F, Cui L, Breeze J, Du X, Wang X, Cong Z, Zhang H, Li B, Hong N, Zhang D. Abnormal anterior cingulum in patients with schizophrenia: a diffusion tensor imaging study. *Neuroreport*. 2003;14(14):1833-1836.
 14. Wang F, Sun Z, Cui L, Du X, Wang X, Zhang H, Cong Z, Hong N, Zhang D. Anterior cingulum abnormalities in male patients with schizophrenia determined through diffusion tensor imaging. *Am J Psychiatry*. 2004;161(3):573-575.
 15. Agartz I, Andersson JL, Skare S. Abnormal brain white matter in schizophrenia: a diffusion tensor imaging study. *Neuroreport*. 2001;12(10):2251-2254.
 16. Ardekani BA, Nierenberg J, Hoptman MJ, Javitt DC, Lim KO. MRI study of white matter diffusion anisotropy in schizophrenia. *Neuroreport*. 2003;14(16):2025-2029.
 17. Foong J, Maier M, Clark CA, Barker GJ, Miller DH, Ron MA. Neuropathological abnormalities of the corpus callosum in schizophrenia: a diffusion tensor imaging study. *J Neurol Neurosurg Psychiatry*. 2000;68(2):242-244.
 18. Hubl D, Koenig T, Strik W, Federspiel A, Kreis R, Boesch C, Maier SE, Schroth G, Lovblad K, Dierks T. Pathways that make voices: white matter changes in auditory hallucinations. *Arch Gen Psychiatry*. 2004;61(7):658-668.
 19. Price G, Bagary MS, Cercignani M, Altmann DR, Ron MA. The corpus callosum in first episode schizophrenia: a diffusion tensor imaging study. *J Neurol Neurosurg Psychiatry*. 2005;76(4):585-587.
 20. Price G, Cercignani M, Parker GJ, Altmann DR, Barnes TR, Barker GJ, Joyce EM, Ron MA. Abnormal brain connectivity in first-episode psychosis: a diffusion MRI tractography study of the corpus callosum. *Neuroimage*. 2007;35(2):458-466.
 21. Burns J, Job D, Bastin ME, Whalley H, Macgillivray T, Johnstone EC, Lawrie SM. Structural disconnectivity in schizophrenia: a diffusion tensor magnetic resonance imaging study. *Br J Psychiatry*. 2003;182:439-443.
 22. Butler PD, Zemon V, Schechter I, Saperstein AM, Hoptman MJ, Lim KO, Revheim N, Silipo G, Javitt DC. Early-stage visual processing and cortical amplification deficits in schizophrenia. *Arch Gen Psychiatry*. 2005;62(5):495-504.
 23. Hao Y, Liu Z, Jiang T, Gong G, Liu H, Tan L, Kuang F, Xu L, Yi Y, Zhang Z. White matter integrity of the whole brain is disrupted in first-episode schizophrenia. *Neuroreport*. 2006;17(1):23-26.
 24. Szaszko PR, Ardekani BA, Ashtari M, Kumra S, Robinson DG, Sevy S, Gunduz-Bruce H, Malhotra AK, Kane JM, Bilder RM, Lim KO. White matter abnormalities in first-episode schizophrenia or schizoaffective disorder: a diffusion tensor imaging study. *Am J Psychiatry*. 2005;162(3):602-605.
 25. Federspiel A, Begre S, Kiefer C, Schroth G, Strik WK, Dierks T. Alterations of white matter connectivity in first episode schizophrenia. *Neurobiol Dis*. 2006;22(3):702-709.
 26. Kumra S, Ashtari M, McMeniman M, Vogel J, Augustin R, Becker DE, Nakayama E, Gyato K, Kane JM, Lim K, Szaszko P. Reduced frontal white matter integrity in early-onset schizophrenia: a preliminary study. *Biol Psychiatry*. 2004;55(12):1138-1145.
 27. Kumra S, Ashtari M, Cervellione KL, Henderson I, Kester H, Roofeh D, Wu J, Clarke T, Thaden E, Kane JM, Rhinewine J, Lencz T, Diamond A, Ardekani BA, Szaszko PR. White matter abnormalities in early-onset schizophrenia: a voxel-based diffusion tensor imaging study. *J Am Acad Child Adolesc Psychiatry*. 2005;44(9):934-941.
 28. Serene JA, Ashtari M, Szaszko P, Kumra S. Neuroimaging studies of children with serious emotional disturbances: a selective review. *Can J Psychiatry*. 2007;52(3):135-145.
 29. Papadakis NG, Xing D, Huang CL, Hall LD, Carpenter TA. A comparative study of acquisition schemes for diffusion tensor imaging using MRI. *J Magn Reson*. 1999;137(1):67-82.
 30. Hollingshead AB. *Four-Factor Index of Social Status*. New Haven, CT: Yale University Dept of Sociology; 1975.
 31. Wilkinson GS. *WRAT3: Wide Range Achievement Test Administration Manual*. Wilmington, DE: Wide Range Inc; 1993.
 32. Rhinewine JP, Lencz T, Thaden EP, Cervellione KL, Burdick KE, Henderson I, Bhaskar S, Keehlisen L, Kane J, Kohn N, Fisch GS, Bilder RM, Kumra S. Neurocognitive profile in adolescents with early-onset schizophrenia: clinical correlates. *Biol Psychiatry*. 2005;58(9):705-712.
 33. Kaufman J, Birmaher B, Brent D, Rao U, Flynn C, Moreci P, Williamson D, Ryan N. Schedule for Affective Disorders and Schizophrenia for School-Age Children—Present and Lifetime Version (K-SADS-PL): initial reliability and validity data. *J Am Acad Child Adolesc Psychiatry*. 1997;36(7):980-988.
 34. Woerner MG, Mannuzza S, Kane JM. Anchoring the BPRS: an aid to improved reliability. *Psychopharmacol Bull*. 1988;24(1):112-117.
 35. Andreasen NC. *Scale for the Assessment of Negative Symptoms (SANS)*. Iowa City: University of Iowa; 1982.
 36. Hales RE, Yudofsky SC. *Textbook of Clinical Neuropsychiatry*. 4th ed. Washington, DC: American Psychiatric Publishing; 2003.
 37. Woods SW. Chlorpromazine equivalent doses for the newer atypical antipsychotics. *J Clin Psychiatry*. 2003;64(6):663-667.
 38. Reese TG, Heid O, Weisskoff RM, Wedeen VJ. Reduction of eddy-current-induced distortion in diffusion MRI using a twice-refocused spin echo. *Magn Reson Med*. 2003;49(1):177-182.
 39. Ardekani BA, Guckemus S, Bachman A, Hoptman MJ, Wojtaszek M, Nierenberg J. Quantitative comparison of algorithms for inter-subject registration of 3D volumetric brain MRI scans. *J Neurosci Methods*. 2005;142(1):67-76.
 40. Ashtari M, Kumra S, Bhaskar SL, Clarke T, Thaden E, Cervellione KL, Rhinewine J, Kane JM, Adesman A, Milanaik R, Maytal J, Diamond A, Szaszko P, Ardekani BA. Attention-deficit/hyperactivity disorder: a preliminary diffusion tensor imaging study. *Biol Psychiatry*. 2005;57(5):448-455.
 41. Basser PJ. Inferring microstructural features and the physiological state of tissues from diffusion-weighted images. *NMR Biomed*. 1995;8(7-8):333-344.
 42. Pierpaoli C, Basser PJ. Toward a quantitative assessment of diffusion anisotropy. *Magn Reson Med*. 1996;36(6):893-906.
 43. Xue R, van Zijl PC, Crain BJ, Solaiyappan M, Mori S. In vivo three-dimensional reconstruction of rat brain axonal projections by diffusion tensor imaging. *Magn Reson Med*. 1999;42(6):1123-1127.
 44. Mori S, Kaufmann WE, Davatzikos C, Stieltjes B, Amodei L, Fredericksen K, Pearlson GD, Melhem ER, Solaiyappan M, Raymond GV, Moser HW, van Zijl PC. Imaging cortical association tracts in the human brain using diffusion-tensor-based axonal tracking. *Magn Reson Med*. 2002;47(2):215-223.
 45. Wakana S, Jiang H, Nagae-Poetscher LM, van Zijl PC, Mori S. Fiber tract-based atlas of human white matter anatomy. *Radiology*. 2004;230(1):77-87.
 46. Okada T, Miki Y, Fushimi Y, Hanakawa T, Kanagaki M, Yamamoto A, Urayama S, Fukuyama H, Hiraoka M, Togashi K. Diffusion-tensor fiber tractography: intra-individual comparison of 3.0-T and 1.5-T MR imaging. *Radiology*. 2006;238(2):668-678.
 47. Kunimatsu A, Aoki S, Masutani Y, Abe O, Hayashi N, Mori H, Masumoto T, Ohtomo K. The optimal trackability threshold of fractional anisotropy for diffusion tensor tractography of the corticospinal tract. *Magn Reson Med Sci*. 2004;3(1):11-17.
 48. Jiang H, van Zijl PC, Kim J, Pearlson GD, Mori S. DTIStudio: resource program for diffusion tensor computation and fiber bundle tracking. *Comput Methods Programs Biomed*. 2006;81(2):106-116.
 49. Pajevic S, Pierpaoli C. Color schemes to represent the orientation of anisotropic tissues from diffusion tensor data: application to white matter fiber tract mapping in the human brain. *Magn Reson Med*. 1999;42(3):526-540.
 50. Sullivan EV, Adalsteinsson E, Pfefferbaum A. Selective age-related degradation of anterior callosal fiber bundles quantified in vivo with fiber tracking. *Cereb Cortex*. 2006;16(7):1030-1039.
 51. Kaplan W. *Advanced Calculus*. 5th ed. Boston, MA: Addison Wesley; 2003.

52. Alexander DC, Pierpaoli C, Basser PJ, Gee JC. Spatial transformations of diffusion tensor magnetic resonance images. *IEEE Trans Med Imaging*. 2001;20(11):1131-1139.
53. Kent JT, Bibby JM, Marida KV. *Multivariate Analysis: Probability and Mathematical Statistics*. San Diego, CA: Academic Press; 1980.
54. Benjamini Y, Hochberg Y. Controlling the false discovery rate: a practical and powerful approach to multiple testing. *J R Stat Soc Ser B*. 1995;57:289-300.
55. Catani M, Jones DK, Donato R, Ffytche DH. Occipito-temporal connections in the human brain. *Brain*. 2003;126(pt 9):2093-2107.
56. Morris JS, Friston KJ, Buchel C, Frith CD, Young AW, Calder AJ, Dolan RJ. A neuromodulatory role for the human amygdala in processing emotional facial expressions. *Brain*. 1998;121(pt 1):47-57.
57. Pessoa L, McKenna M, Gutierrez E, Ungerleider LG. Neural processing of emotional faces requires attention. *Proc Natl Acad Sci U S A*. 2002;99(17):11458-11463.
58. Ross ED. Sensory-specific and fractional disorders of recent memory in man: I. Isolated loss of visual recent memory. *Arch Neurol*. 1980;37(4):193-200.
59. Narr KL, Toga AW, Szeszko P, Thompson PM, Woods RP, Robinson D, Sevy S, Wang Y, Schrock K, Bilder RM. Cortical thinning in cingulate and occipital cortices in first episode schizophrenia. *Biol Psychiatry*. 2005;58(1):32-40.
60. Song SK, Yoshino J, Le TQ, Lin SJ, Sun SW, Cross AH, Armstrong RC. Demyelination increases radial diffusivity in corpus callosum of mouse brain. *Neuroimage*. 2005;26(1):132-140.
61. Uranova N, Orlovskaya D, Vikhreva O, Zimina I, Kolomeets N, Vostrikov V, Rachmanova V. Electron microscopy of oligodendroglia in severe mental illness. *Brain Res Bull*. 2001;55(5):597-610.
62. Benes FM, Turtle M, Khan Y, Farol P. Myelination of a key relay zone in the hippocampal formation occurs in the human brain during childhood, adolescence, and adulthood. *Arch Gen Psychiatry*. 1994;51(6):477-484.
63. Barnea-Goraly N, Menon V, Eckert M, Tamm L, Bammer R, Karchemskiy A, Dant CC, Reiss AL. White matter development during childhood and adolescence: a cross-sectional diffusion tensor imaging study. *Cereb Cortex*. 2005;15(12):1848-1854.
64. Kovacs I, Kozma P, Feher A, Benedek G. Late maturation of visual spatial integration in humans. *Proc Natl Acad Sci U S A*. 1999;96(21):12204-12209.
65. Neville H, Bavelier D. Human brain plasticity: evidence from sensory deprivation and altered language experience. *Prog Brain Res*. 2002;138:177-188.
66. Kovacs I. Human development of perceptual organization. *Vision Res*. 2000;40(10-12):1301-1310.
67. Dworkin RH, Lewis JA, Cornblatt BA, Erlenmeyer-Kimling L. Social competence deficits in adolescents at risk for schizophrenia. *J Nerv Ment Dis*. 1994;182(2):103-108.
68. Brune M. Emotion recognition, "theory of mind," and social behavior in schizophrenia. *Psychiatry Res*. 2005;133(2-3):135-147.
69. Mueser KT, Doonan R, Penn DL, Blanchard JJ, Bellack AS, Nishith P, DeLeon J. Emotion recognition and social competence in chronic schizophrenia. *J Abnorm Psychol*. 1996;105(2):271-275.
70. Penn DL, Spaulding W, Reed D, Sullivan M. The relationship of social cognition to ward behavior in chronic schizophrenia. *Schizophr Res*. 1996;20(3):327-335.
71. McKenna K, Gordon CT, Lenane M, Kaysen D, Fahey K, Rapoport JL. Looking for childhood-onset schizophrenia: the first 71 cases screened. *J Am Acad Child Adolesc Psychiatry*. 1994;33(5):636-644.
72. Diederich NJ, Goetz CG, Stebbins GT. Repeated visual hallucinations in Parkinson's disease as disturbed external/internal perceptions: focused review and a new integrative model. *Mov Disord*. 2005;20(2):130-140.